Journal of Organometallic Chemistry 887 (2019) 71–79

Contents lists available at ScienceDirect

Journal of Organometallic Chemistry

journal homepage: www.elsevier.com/locate/jorganchem

Communication

Synthesis, characterization and antitumor activity of (*E*)-2-methyl-3-ferrocenyl-*N*-acrylamide derivatives

Yan-Wei Liu [a], Hui-Jie Cheng [c], Ban-Feng Ruan [c, *], Qiao Hu [b, **]

[a] Department of General Surgery, Taihe Hospital, Hubei University of Medicine, Shiyan, 442000, China
[b] Department of Infection Control, Taihe Hospital, Hubei University of Medicine, Shiyan, 442000, China
[c] School of Biological and Medical Engineering, Hefei University of Technology, Hefei, 230009, China

ARTICLE INFO

Article history:
Received 28 January 2019
Received in revised form
25 February 2019
Accepted 26 February 2019
Available online 5 March 2019

Keywords:
Ferrocene
Amide derivative
X-ray structural analysis
Antitumor activity
Cell apoptosis

ABSTRACT

We report here the synthesis, characterization of seventeen (*E*)-2-methyl-3-ferrocenyl-*N*-acrylamides. The single crystal structures of the key intermediate **b** and two target compounds **d5** and **d6** were confirmed by X-ray crystallographic analysis. Antitumor activity of all compounds was tested *in vitro*. Compound **d1** was the most significant one against B16−F10 cell line, indicating that it could be a good candidate for further study. Furthermore, cancer cell apoptosis assay was performed and the result indicated that compound **d1** effectively fueled B16−F10 cells apoptosis in a dose-dependent manner.

1. Introduction

Great efforts have been contributed to the development of new transition metal-based drugs [1–5]. In 1985, Top et al. introduced the concept “bioorganometallic chemistry” to describe any compound with a metal-carbon bond with a biological function whether naturally occurring or synthetic [6]. This kind of compounds is generally known as organometallic compounds. Among them, ferrocene is a representative organometallic compound with two Cp (cyclopentadienyl) rings bound on opposite sides of the central Fe atom. Ferrocene and its derivatives usually are not toxic compounds and are robust, lipophilic, and have good redox properties [7]. For these reasons, a large number of ferrocenyl compounds with potent antitumor [8,9], antimalarial [10,11], antifungal [12,13], DNA-cleaving activities [14,15] and the inhibitory effects on Alzheimer's disease [16,17] had been reported. In 2012, Biot and his coworker had reviewed the development and recent advances on the preparation of ferrocenic compounds as a new class of antimalarial agents with potential for clinical development [18]; In 2015, Jaouen et al. had reviewed the ferrocifen type anti-cancer drugs [19]; In 2017, Malay Patra and Gilles Gasser had published a perspective which delineated strategies for the systematic incorporation offerrocenyl groups into known drugs or drug candidates, with a view to finding new drug leads. They also provided a critical evaluation of the difficulties associated with obtaining the clinical approval that would enable ferrocene-containing molecules to transition from being synthetic curiosities to effective drugs [20]; In 2018, Kowalski had delineated potential of ferrocenyl secondary natural product conjugates in medicinal chemistry e.g., as antimicrobial, antiparasite and anticancer agents [21].

Given that bioactive compounds with amide moiety have more potential druggability, many researchers have pay great attention to the biological activities of different amide derivatives of ferrocene [22–29]. Our group have also designed, synthesized and evaluated the *in vitro* antitumor activities of several different series of ferrocene derivatives in the past few years [30–32]. Among them, some compounds exhibited potent antitumor activities against a panel of cancer cell lines. Meanwhile, our group have also published several series of cinnamamide, 2-cyanophenylacrylamide and phenyl acrylate derivatives of resveratrol. Some target compounds exhibited potent antitumor and antiinflammation activities in the past years [33–35]. To extend our research range, we have been trying to build a compound library which aims to collect a large number of small molecular

* Corresponding author.
** Corresponding author.
E-mail addresses: ruanbf@hfut.edu.cn (B.-F. Ruan), mili0487@sina.com (Q. Hu).

https://doi.org/10.1016/j.jorganchem.2019.02.021
0022-328X/

compounds bearing variety of phenylacrylamide moieties for activities screening. In this work, we reported the synthesis, characterization and biological evaluation of a novel series of novel (*E*)-2-methyl-3-ferrocenyl-*N*-acrylamide derivatives. Among them, the crystal structures of the intermediate **b** and two title compounds **d5** and **d6** were confirmed by X-ray crystallographic analysis.

2. Experimental

2.1. General

All the chemicals used were commercial products employed as received. Column chromatography was performed using silica gel 60 (40–60 μm). The solvents for chromatography were used without purification. The reactions were monitored by TLC on Silica Gel 60F-254 plates with detection by UV light. The NMR solvents $CDCl_3$ and DMSO-d_6 were purchased from Sigma. NMR spectra were recorded on a 400 and or 600 MHz instrument at room temperature and the chemical shift was reported relatively to the frequency of TMS protons. ESI-MS spectra were recorded on a Mariner System 5304 Mass spectrometer. Element analysis were measured with a CHN–O-Rapid instrument and were within ±0.4% of the theoretical values.

2.2. Synthesis

The synthesis of all the title compounds (**d1-17**) were carried out as shown in Scheme 1. Compounds (*E*)-ethyl 2-methyl-3-ferrocenylacrylate (**b**) and (*E*)-2-methyl-3-ferrocenylacrylic acid (**c**) were made according to the previous reported methods.

2.2.1. Ethyl (E)-2-methyl-3-ferrocenylacrylate (*b*)

A mixture of ferrocenecarboxaldehyde (**a**) (5.35 g, 25.0 mmol) in DMF (100 mL) was added ethyl 2-(triphenylphosphoranylidene) propionate (11.35 g, 32.5 mmol). The mixture was refluxed for 6 h. The solvent was evaporated under reduce pressure. The residue was purified by column chromatography using silica gel (Petroleum ether/Ethyl acetate = 6:1, V/V). Brown solid (yield 84.8%), m.p: 59–61 °C. ^{1}H NMR (600 MHz, $CDCl_3$): δ 7.44 (s, 1H, C=CH), 4.49 (s, 2H, Fc), 4.36 (s, 2H, Fc), 4.23 (q, J = 7.1 Hz, 2H, CH_2), 4.14 (s, 5H, Fc), 2.02 (s, 3H, CH_3), 1.33 (t, J = 7.1 Hz, 3H, CH_3).

2.2.2. (E)-2-Methyl-3-ferrocenylacrylic acid (*c*)

A solution of **b** (2.98 g, 1.0 mmol) and sodium hydroxide (0.4 g, 10 mmol) in 100 mL of ethanol and 20 mL water was refluxed for 4 h. After removal of the solvent, the residue was added 50 mL of cold water and adjusted the pH to 2.0 with 1.0 M HCl. The precipitate was removed, washed with water and dried. Brown solid (yield 92.3%), m.p: 165–167 °C. ^{1}H NMR (600 MHz, $CDCl_3$): δ 7.60 (s, 1H, C=CH), 4.54 (s, 2H, Fc), 4.41 (s, 2H, Fc), 4.16 (s, 5H, Fc), 2.04 (s, 3H, CH_3).

2.2.3. General procedure for the synthesis of compounds *d1-17*

A mixture of **c** (0.324 g, 1.2 mmol), 3-(ethyliminomethylideneamino)-*N*, *N*-dimethylpropan-1-ami,hydrochloride (EDCI) (0.23 g, 1.2 mmol) and 1-Hydroxybenzotriazole (HOBt) (0.135 g, 1 mmol) in 10 mL of CH_2Cl_2 was stirred at room temperature for 0.5 h. Then, appropriate amines (1.0 mmol) in dry CH_2Cl_2 (10 mL) was added dropwise. The reaction mixture was stirred overnight at room temperature. When the reaction was completed as monitored by TLC, the solvent was removed. The residue was purified by silica gel chromatography using petroleum ether/ethyl acetate as eluent to obtain target compounds **d1-17**, see Table 1.

*2.2.3.1. (E)-2-Methyl-3-ferrocenyl-N-phenylacrylamide (**d1**).* Redish-brown solid (64.7%, yield), m.p. 146–148 °C, ^{1}H NMR (400 MHz, DMSO-d_6): δ 9.60 (s, 1H, NH), 7.69–7.71 (d, J = 8.0 Hz, 2H, Ar), 7.29–7.33 (t, J = 8.0 Hz, 2H, Ar), 7.12 (s, 1H, C=CH), 7.04–7.08 (t, J = 8.0 Hz, 1H, Ar), 4.55 (s, 2H, Fc), 4.40 (s, 2H, Fc), 4.19 (s, 5H, Fc), 2.05 (s, 3H, CH_3). ^{13}C NMR (151 MHz, DMSO-d_6) δ 171.0 (O = *C), 142.5136.0, 131.5, 126.3, 123.4, 82.8, 73.2, 72.7, 72.2, 17.7 (-C=C-*CH_3). MS (ESI): 344.1 ($C_{20}H_{19}FeNO$, [M-H]$^-$). Anal. Calc. for $C_{20}H_{19}FeNO$:C,70.41; H, 6.71; O, 4.26%. Found: C,70.49; H, 6.73; O, 4.24%.

*2.2.3.2. (E)-2-Methyl-3- ferrocenyl -N-(p-tolyl)acrylamide (**d2**).* Redish-brown solid (73.6%, yield), m.p. 135–137 °C, ^{1}H NMR (400 MHz, DMSO-d_6): δ 9.55 (s, 1H, NH), 7.57–7.58 (d, J = 4.0 Hz, 2H, Ar), 7.13 (s, 1H, C=CH), 7.09–7.11 (d, J = 8.0 Hz, 2H, Ar), 4.55 (s, 2H, Fc), 4.40 (s, 2H, Fc), 4.19 (s, 5H, Fc), 2.26 (s, 3H, Ar–CH_3), 2.03 (s, 3H, C–CH_3). ^{13}C NMR (151 MHz, DMSO-d_6): δ 170.2 (O = *C), 138.3, 136.7, 136.4, 132.1, 130.4, 122.8, 82.5, 73.0, 72.7, 72.1, 23.6 (Ar–*CH_3), 17.2 (-C=C-*CH_3). MS (ESI): 358.1 ($C_{21}H_{21}FeNO$, [M-H]$^-$). Anal. Calc. for $C_{21}H_{21}FeNO$: C, 70.96; H, 6.99; O, 4.11%. Found: C, 71.04; H, 7.01; O, 4.12%.

*2.2.3.3. (E) -2-Methyl-3-ferrocenyl-N-(m-tolyl)acrylamidec (**d3**).* Redish-brown solid (67.8%, yield), m.p. 142–144 °C, ^{1}H NMR (400 MHz, DMSO-d_6): δ 9.52 (s, 1H, NH), 7.50–7.52 (d, J = 8.0 Hz, 2H, Ar), 7.17–7.21 (t, J = 8.0 Hz, 1H, Ar), 7.11 (s, 1H, C=CH), 6.87–6.89 (d, J = 8.0 Hz, 1H, Ar), 4.55 (s, 2H, Fc), 4.40 (s, 2H, Fc), 4.19 (s, 5H, Fc), 2.29 (s, 3H, Ar–CH_3), 2.04 (s, 3H, C–CH_3).^{13}C NMR (151 MHz, $CDCl_3$): δ 170.3 (O = *C), 141.6, 140.7, 137.0, 131.5, 130.4, 127.6, 125.9, 123.3, 119.7, 82.2, 73.0, 72.6, 72.0, 24.2 (Ar–*CH_3), 17.1 (-C=C-*CH_3). MS(ESI): 359.3($C_{21}H_{21}FeNO$). Anal. Calc. for: $C_{21}H_{21}FeNO$: C, 70.96; H, 6.99; O, 4.11%. Found: C, 70.92; H, 7.01; O, 4.12%.

*2.2.3.4. (E)-N-(4-methoxyphenyl)-2-methyl-3-ferrocenylacrylamide (**d4**).* Reddish-yellow solid (75.8%, yield), m.p. 153–155 °C, ^{1}H NMR (400 MHz, DMSO-d_6): δ 9.62 (s, 1H, NH), 7.40 (s, 1H), 7.28–7.30 (d, J = 8.0 Hz, 1H, Ar), 7.19–7.23 (t, J = 8.0 Hz, 1H, Ar), 7.10 (s, 1H, C=CH), 6.63–6.65 (d, J = 8.0 Hz, 1H, Ar), 4.56 (s, 2H, Fc), 4.41 (s, 2H, Fc), 4.19 (s, 5H, Fc), 3.74 (s, 3H, OCH_3), 2.04 (s, 3H, C–CH_3). ^{13}C NMR (151 MHz, $CDCl_3$): δ 170.3 (O = *C), 141.6, 140.8, 137.0, 131.5, 130.4,

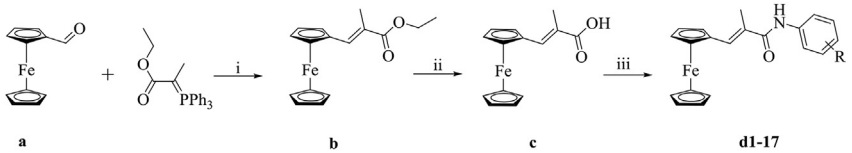

d1: R = H; **d2**: R = 4-CH_3; **d3**: R = 3-CH_3; **d4**: R = 4-OCH_3; **d5**: R = 3-OCH_3; **d6**: R = 4-F; **d7**: R = 3-F; **d8**: R = 4-Cl; **d9**: R = 3-Cl; **d10**: R = 4-Br; **d11**: R = 3-Br; **d12**: R = 4-CF_3; **d13**: R = 3-CF_3; **d14**: R = 4-OCF_3; **d15**: R = 3-OCF_3; **d16**: R = 3,5-di-CH_3; **d17**: R = 3,5-di-OCH_3.

Scheme 1. Synthesis of compounds **d1-17**.
Reagent and conditions: (i) DCM, reflux, 6 h; (ii) EtOH/H_2O, NaOH, reflux, 4 h; (iii) substituted anilines, DCM, EDCI/HOBt, reflux, overnight.

Table 1
Chemical structures of the title compounds d1-17.

Structure	Comp. no.	R	Comp. no.	R
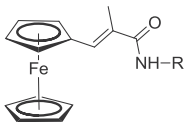	**d1**		**d2**	
	d3		**d4**	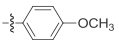
	d5	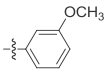	**d6**	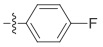
	d7		**d8**	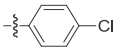
	d9		**d10**	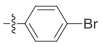
	d11		**d12**	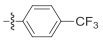
	d13		**d14**	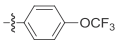
	d15		**d16**	
	d17			

127.6, 123.4, 119.8, 82.2, 73.0, 72.6, 72.0, 24.2 (-O*CH_3), 17.2 (-C═C-*CH_3). MS (ESI): 376.3 ($C_{21}H_{21}FeNO_2$, $[M+H]^+$). Anal. Calc. For $C_{21}H_{21}FeNO_2$: C, 68.16; H, 6.71; O, 7.89%. Found: C, 68.10; H, 6.69; O, 7.86%.

*2.2.3.5. (E)-N-(3-methoxyphenyl)-2-methyl-3-ferrocenylacrylamide (**d5**).* Reddish-yellow solid (68.3%, yield), m.p. 155–157 °C, ^{1}H NMR (400 MHz, DMSO-d_6): δ 9.63 (s, 1H, NH), 7.42 (s, 1H, Ar), 7.30–7.32 (d, J = 8.0 Hz, 1H, Ar), 7.19–7.23 (t, J = 8.0 Hz, 1H, Ar), 7.11 (s, 1H, C═CH), 6.63–6.65 (d, J = 8.0 Hz, 1H, Ar), 4.55 (s, 2H, Fc), 4.40 (s, 2H, Fc), 4.18 (s, 5H, Fc), 3.74 (s, 3H, OCH_3), 2.04 (s, 3H, C–CH_3).^{13}C NMR (151 MHz, $CDCl_3$): δ 170.3 (O = *C), 162.8, 142.1, 137.3, 132.3, 130.2, 114.7, 113.0, 108.1, 82.1, 73.0, 72.7, 72.0, 58.0, 17.1 (-C═C-*CH_3). MS (ESI): 375.3 ($C_{21}H_{21}FeNO_2$). Anal. Calc. For $C_{21}H_{21}FeNO_2$: C, 68.16; H, 6.71; O, 7.89%. Found: C,68.14; H, 6.70; O, 7.90%.

*2.2.3.6. (E)-N-(4-fluorophenyl)-2-methyl-3-ferrocenylacrylamide (**d6**).* Redish-brown solid (61.4%, yield), m.p. 180–182 °C, ^{1}H NMR (400 MHz, DMSO-d_6): δ 9.70 (s, 1H, NH), 7.69–7.73 (t, J = 8.0, 2H, Ar), 7.14–7.18 (t, J = 8.0 Hz, 2H, Ar), 7.11 (s, 1H, C═CH), 4.56 (s, 2H, Fc), 4.41 (s, 2H, Fc), 4.19 (s, 5H, Fc), 2.04 (s, 3H, C–CH_3). ^{13}C NMR (151 MHz, $CDCl_3$): δ 170.3 (O = *C), 162.8, 161.2, 137.4, 136.9, 129.9, 124.6, 118.4, 118.2, 82.1, 73.0, 72.7, 72.0, 17.1 (-C═C-*CH_3). MS (ESI): 362.1 ($C_{21}H_{18}FFeNO$, $[M-H]^-$). Anal. Calc. for $C_{21}H_{18}FFeNO$: C, 67.19; H, 6.15; O, 4.07%. Found: C, 67.24; H, 6.13; O, 4.11%.

*2.2.3.7. (E)-N-(3-fluorophenyl)-2-methyl-3-ferrocenylacrylamide (**d7**).* Redish-brown solid (57.8%, yield), m.p. 151–153 °C,^{1}H NMR (400 MHz, DMSO-d_6): δ 9.83 (s, 1H, NH), 7.68–7.71 (d, J = 12.0 Hz, 1H, Ar), 7.48–7.50 (d, J = 8.0 Hz, 1H, Ar), 7.32–7.38 (dd, J = 16.0, 8.0 Hz, 1H, Ar), 7.13 (s, 1H, C═CH), 6.88 (t, J = 8.0 Hz, 1H, Ar), 4.57 (s, 2H, Fc), 4.42 (s, 2H, Fc), 4.20 (s, 5H, Fc), 2.04 (s, 3H, C–CH_3). ^{13}C NMR (151 MHz, $CDCl_3$): δ 170.2 (O = *C), 166.5, 142.5, 137.7, 132.7, 129.8, 126.9, 117.8, 113.6, 113.4, 110.2, 110.0, 81.9, 73.0, 72.8, 72.0, 17.1 (-C═C-*CH_3). MS (ESI): 362.2 ($C_{21}H_{18}FFeNO$, $[M-H]^-$). Anal. Calc. for $C_{21}H_{18}FFeNO$: C, 67.19; H, 6.15; O, 4.07%. Found: C, 67.14; H, 6.13; O, 4.04%.

*2.2.3.8. (E)-N-(4-chlorophenyl)-2-methyl-3-ferrocenylacrylamide (**d8**).* Redish-brown solid (60.9%, yield), m.p. 169–170 °C, ^{1}H NMR (400 MHz, DMSO-d_6): δ 9.77 (s, 1H, NH), 7.74–7.76 (d, J = 8.0 Hz, 2H, Ar), 7.36–7.38 (d, J = 8.0 Hz, 2H, Ar), 7.13 (s, 1H, C═CH), 4.56 (s, 2H, Fc), 4.41 (s, 2H, Fc), 4.19 (s, 5H, Fc), 2.04 (s, 3H, C–CH_3). ^{13}C NMR (151 MHz, DMSO-d_6): δ 171.1 (O = *C), 141.6, 136.4, 131.5, 131.4, 129.8, 124.8, 82.6, 73.2, 72.8, 72.2, 17.7 (-C═C-*CH_3). MS (ESI): 378.2 ($C_{21}H_{18}ClFeNO$, $[M-H]^-$). Anal. Calc. for $C_{21}H_{18}ClFeNO$: C, 64.49; H, 5.90; O, 3.90%. Found: C, 64.57; H, 5.92; O, 3.88%.

*2.2.3.9. (E)-N-(3-chlorophenyl)-2-methyl-3-ferrocenylacrylamide (**d9**).* Redish-brown solid (57.3%, yield), m.p. 126–128 °C, ^{1}H NMR (400 MHz, DMSO-d_6): δ 9.77 (s, 1H, NH), 7.89 (s, 1H, Ar), 7.64–7.66 (d, J = 8.0 Hz, 1H, Ar), 7.32–7.36 (t, J = 8.0 Hz, 1H), 7.14 (s, 1H, C═CH), 7.10–7.12 (d, J = 8.0 Hz, 1H, Ar), 4.57 (s, 1H, Fc), 4.42 (s, 2H, Fc), 4.19 (s, 5H, Fc), 2.04 (s, 3H, C–CH_3). ^{13}C NMR (151 MHz, DMSO-d_6): δ 171.2 (O = *C), 144.1, 136.7, 135.9, 133.2, 131.2, 125.9, 122.7, 121.6, 82.6, 73.3, 72.9, 72.2, 17.6 (-C═C-*CH_3). MS (ESI): 378.1 ($C_{21}H_{18}ClFeNO$, $[M-H]^-$). Anal. Calc. for $C_{21}H_{18}ClFeNO$: C, 64.49; H, 5.90; O, 3.90%. Found: C, 64.53; H, 5.90; O, 3.87%.

*2.2.3.10. (E)-N-(4-bromophenyl)-2-methyl-3-ferrocenylacrylamide (**d10**).* Reddish-yellow solid (61.4%, yield), m.p. 180–181 °C, ^{1}H NMR (400 MHz, DMSO-d_6): δ 9.77 (s, 1H, NH), 7.68–7.70 (d, J = 8.0 Hz, 2H, Ar), 7.49–7.51 (d, J = 8.0 Hz, 2H, Ar), 7.12 (s, 1H, C═CH), 4.57 (s, 2H, Fc), 4.41 (s, 2H, Fc), 4.19 (s, 5H, Fc), 2.04 (s, 3H, C–CH_3). ^{13}C NMR (151 MHz, $CDCl_3$): δ 170.2 (O = *C), 140.0, 137.7, 134.6, 129.8, 124.2, 119.3, 82.0, 73.0, 72.8, 72.0, 17.1 (-C═C-*CH_3). MS

(ESI): 425.1 ($C_{21}H_{18}BrFeNO$, $[M+H]^+$). Anal. Calc. for $C_{21}H_{18}BrFeNO$: C, 58.18; H, 5.33; O, 3.52%. Found: C, 58.12; H, 5.30; O, 3.54%.

*2.2.3.11. (E)-N-(3-bromophenyl)-2-methyl-3-ferrocenylacrylamide (**d11**).* Reddish-yellow solid (55.4%, yield), m.p. 129–132 °C, ^{1}H NMR (400 MHz, DMSO-d_6): δ 9.79 (s, 1H, NH), 8.03 (s, 1H, Ar), 7.70–7.71 (d, J = 4.0 Hz, 1H), 7.27–7.31 (t, J = 8.0, 1H, Ar), 7.24–7.25 (d, J = 4.0 Hz, 1H, Ar), 7.14 (s, 1H, C═CH), 4.57 (s, 2H, Fc), 4.42 (s, 2H, Fc), 4.19 (s, 5H, Fc), 2.04 (s, 3H, C–CH_3). ^{13}C NMR (151 MHz, $CDCl_3$): δ 170.4 (O = *C), 142.2, 137.8, 132.9, 129.8, 129.7, 125.6, 125.3, 121.1, 82.0, 73.0, 72.8, 72.0, 17.1 (-C═C-*CH_3). MS (ESI): 425.2 ($C_{21}H_{18}BrFeNO$, $[M+H]^+$). Anal. Calc. for $C_{21}H_{18}BrFeNO$: C, 58.18; H, 5.33; O, 3.52%. Found: C, 58.11; H, 5.30; O, 3.55%.

*2.2.3.12. (E)-2-Methyl-3-ferrocenyl-N-(4-(trifluoromethyl)phenyl) acrylamide (**d12**).* Reddish-yellow oil (62.3%, yield), ^{1}H NMR (400 MHz, DMSO-d_6): δ 9.96 (s, 1H, NH), 7.94–7.96 (d, J = 8.0 Hz, 2H, Ar), 7.67–7.69 (d, J = 8.0 Hz, 2H, Ar), 7.19 (s, 1H, C═CH), 4.57 (s, 2H, Fc), 4.42 (s, 2H, Fc), 4.19 (s, 5H, Fc), 2.06 (s, 3H, C–CH_3). ^{13}C NMR (151 MHz, $CDCl_3$): δ 170.4 (O = *C), 144.0, 138.2, 129.6, 128.9, 122.2, 81.8, 73.1, 72.9, 72.0, 17.1 (-C═C-*CH_3). MS (ESI): 412.2 ($C_{21}H_{18}F_3FeNO$, $[M-H]^-$). Anal. Calc. for $C_{21}H_{18}F_3FeNO$: C, 62.32; H, 5.46; O, 3.61%. Found:C, 62.36; H, 5.48; O, 3.60%.

*2.2.3.13. (E)-2-Methyl-3-ferrocenyl-N-(4-(trifluoromethyl)phenyl) acrylamide (**d13**).* Redish-brown solid (67.3%, yield), m.p. 115–117 °C, ^{1}H NMR (400 MHz, DMSO-d_6): δ 9.94 (s, 1H, NH), 8.18 (s, 1H, Ar), 8.00–8.02 (d, J = 8.0 Hz, 1H, Ar), 7.53–7.57 (t, J = 8.0 Hz, 1H, Ar), 7.38–7.40 (d, J = 8.0 Hz, 1H, Ar), 7.19 (s, 1H, C═CH), 4.57 (s, 2H, Fc), 4.42 (s, 2H, Fc), 4.20 (s, 5H, Fc), 2.07 (s, 3H, C–CH_3). ^{13}C NMR (151 MHz, $CDCl_3$): δ 170.6 (O = *C), 141.5, 138.1, 132.1, 129.6, 125.8, 123.3, 119.5, 81.8, 73.1, 72.9, 72.0, 17.1 (-C═C-*CH_3). MS (ESI): 412.1 ($C_{21}H_{18}F_3FeNO$, $[M-H]^-$). Anal. Calc. for $C_{21}H_{18}F_3FeNO$: C, 62.32; H, 5.46; O, 3.61%. Found: C, 62.25; H, 5.43; O, 3.64%.

*2.2.3.14. (E)-2-Methyl-3–ferrocenylN-(4-(trifluoromethoxy)phenyl) acrylamide (**d14**).* Reddish-yellow solid (74.6%, yield), m.p. 128–130 °C, ^{1}H NMR (400 MHz, DMSO-d_6): δ 9.84 (s, 1H, NH), 7.82–7.83 (d, J = 4.0 Hz, 2H, Ar), 7.34 (s, 2H, Ar), 7.14 (s, 1H, C═CH), 4.57 (s, 2H, Fc), 4.42 (s, 2H, Fc), 4.19 (s, 5H, Fc), 2.05 (s, 3H, C–CH_3). ^{13}C NMR (151 MHz, $CDCl_3$): δ 170.3 (O = *C), 147.8, 139.6, 137.8, 129.8, 124.4, 123.8, 122.3, 81.9, 73.0, 72.8, 72.0, 17.1 (-C═C-*CH_3). MS (ESI): 428.1 ($C_{21}H_{18}F_3FeNO_2$, $[M-H]^-$). Anal. Calc. for $C_{21}H_{18}F_3FeNO_2$: C, 60.15; H, 5.27; O, 6.97%. Found: C, 60.23; H, 5.29; O, 7.00%.

*2.2.3.15. (E)-2-Methyl-3-ferrocenyl-N-(4-(trifluoromethoxy)phenyl) acrylamide (**d15**).* Reddish-yellow solid (69.9%, yield), m.p. 110–112 °C, ^{1}H NMR (400 MHz, DMSO-d_6): δ 9.92 (s, 1H, NH), 7.89 (s, 1H, Ar), 7.70–7.72 (d, J = 8.0 Hz, 1H, Ar), 7.43–7.47 (t, J = 8.0 Hz, 1H, Ar), 7.16 (s, 1H, C═CH), 7.03–7.05 (d, J = 8.0 Hz, 1H, Ar), 4.58 (s, 2H, Fc), 4.42 (s, 2H, Fc), 4.20 (s, 5H, Fc), 2.05 (s, 3H, C–CH_3). ^{13}C NMR (151 MHz, DMSO-d_6): δ 171.3 (O = *C), 151.5, 144.3, 136.9, 133.2, 131.2, 121.8, 118.2, 115.2, 82.5, 73.3, 72.9, 72.2, 17.6 (-C═C-*CH_3). MS (ESI): 429.3 ($C_{21}H_{18}F_3FeNO_2$). Anal. Calc. for $C_{21}H_{18}F_3FeNO_2$: C, 60.15; H, 5.27; O, 6.97%. Found: C, 60.10; H, 5.25; O, 6.93%.

*2.2.3.16. (E)-N-(3,5-dimethylphenyl)-2-methyl-3-ferrocenylacrylamide (**d16**).* Reddish-yellow solid (54.3%, yield), m.p. 181–182 °C, ^{1}H NMR (400 MHz, DMSO-d_6): δ 9.43 (s, 1H, NH), 7.33 (s, 2H, Ar), 7.09 (s, 1H, C═CH), 6.70 (s, 1H, Ar), 4.54 (s, 2H, Fc), 4.40 (s, 2H, Fc), 4.19 (s, 5H, Fc), 2.25 (s, 6H, Ar–CH_3), 2.02 (s, 3H, C–CH_3). ^{13}C NMR (151 MHz, $CDCl_3$): δ 170.2 (O = *C), 141.4, 140.6, 136.8, 130.4, 128.6, 120.4, 82.2, 72.9, 72.6, 72.0, 24.1, 17.1 (-C═C-*CH_3). MS (ESI): 374.3 ($C_{22}H_{23}FeNO$, $[M+H]^+$). Anal. Calc. for $C_{22}H_{23}FeNO$: C, 71.47; H, 7.25; O, 3.97%. Found: C, 71.38; H, 7.21; O, 3.95%.

*2.2.3.17. (E)-N-(3,5-dimethoxyphenyl)-2-methyl-3-ferrocenylacrylamide (**d17**).* Redish-brown solid (52.1%, yield), m.p. 134–136 °C, ^{1}H NMR (400 MHz, DMSO-d_6): δ 9.46 (s, 1H, NH), 7.40 (s, 1H, Ar), 7.25–7.27 (d, J = 8.0 Hz, 1H, Ar), 7.10 (s, 1H, C═CH), 6.89–6.91 (d, J = 8.0 Hz, 1H, Ar), 4.55 (s, 2H, Fc), 4.40 (s, 2H, Fc), 4.19 (s, 5H, Fc), 3.74 (s, 3H, OCH_3), 3.73 (s, 3H, OCH_3), 2.04 (s, 3H, C–CH_3). ^{13}C NMR (151 MHz, $CDCl_3$): δ 170.2 (O = *C), 151.7, 148.4, 137.1, 134.6, 130.1, 114.6, 113.9, 107.7, 82.2, 73.0, 72.6, 72.0, 58.8, 58.5, 17.1 (-C═C-*CH_3). MS (ESI): 406.3 ($C_{22}H_{23}FeNO$, $[M+H]^+$). Anal. Calc. for $C_{22}H_{23}FeNO_3$: C, 66.21; H, 6.71; O, 11.03%. Found: C, 66.26; H, 6.74; O, 11.06%.

2.3. Crystal structure determination

Single crystals of compounds **b**, **d5** and **d6** were obtained by the slow evaporation of dichloromethane/methanol solutions at room temperature. The X-ray single-crystal diffraction for compounds **b, d5** and **d6** were collected on a Siemens Smart 1000 CCD diffractometer equipped with a graphite crystal monochromator situated in the incident beam for data collection at room temperature. The determination of unit cell parameters and data collections were performed with Mo $K\alpha$ radiation (λ = 0.71073 Å). Unit cell dimensions were obtained with least-squares refinements, and all structures were solved by direct methods with SHELXL-97 [36]. All the non-hydrogen atoms were in successive difference Fourier syntheses. The final refinement was performed by full matrix least-squares methods with anisotropic thermal parameters for non-hydrogen atoms on F^2. The hydrogen atoms were added theoretically and riding on the concerned atoms. The crystal data and structure refinement were listed in Table 2. The characteristic bond lengths (Å) and angles (°) were listed in Table 3.

2.4. Antitumor test

The antitumor activity of all the prepared compounds against B16–F10 (mouse melanoma cell line) and A549 (human non-small cell lung cancer cell line) were evaluated as described elsewhere with some modifications [37]. Target tumor cell lines were grown to log phase in RPMI 1640 medium supplemented with 10% fetal bovine serum. After diluting to 2×10^4 cells mL^{-1} with the complete medium, 100 μL of the obtained cell suspension was added to each well of 96-well culture plates. The subsequent incubation was permitted at 37 °C, 5% CO_2 atmosphere for 24 h before the cytotoxicity assessments. Tested samples at pre-set concentrations were added to 6 wells with celecoxib coassayed as positive control. After 72 h exposure period, 100 μL of PBS containing 0.5 mg/mL of MTT (3-(4,5-dimethylthiazol-2-yl)-2,5-diphenyltetrazolium bromide) was added to each well. 4 h later, 100 μL extraction solution (10% SDS-5% isobutyl alcohol-0.01 M HCl) was added. After an overnight incubation at 37 °C, the optical density was measured at a wavelength of 570 nm on an ELISA microplate reader. In all experiments three replicate wells were used for each drug concentration. Each assay was carried out at least three times. The results were summarized in Table 4.

2.5. Analysis of apoptosis

Approximately 10^4 B16–F10 cells/well were plated in a 12 well plate and allowed to adhere. After 12 h, the medium was replaced with fresh culture medium containing compound **d1** at final concentrations of 0, 2 μM, 4 μM, 8 μM and 16 μM. Then cells were harvested after 24 h. They were trypsinized, washed in PBS and

Table 2
Crystallographic data and structure refinements for compounds **b**, **d5** and **d6.**

	b	d5	d6
Formula	$C_{16}H_{18}FeO_2$	$C_{21}H_{21}FeNO_2$	$C_{20}H_{18}FFeNO$
Mr	298.15	375.24	363.20
Crystal system	Monoclinic	Monoclinic	Monoclinic
Space group	$P2_1/c$	$P2_1/c$	$P2_1/n$
Crystal size (mm^3)	$0.37 \times 0.34 \times 0.31$	$0.34 \times 0.21 \times 0.2$	$0.23 \times 0.15 \times 0.02$
a (Å)	18.578(2)	10.8033(4)	11.8695(3)
b (Å)	7.4195(7)	16.8610(5)	16.6565(7)
c (Å)	10.4566(8)	10.1419(3)	24.7367(8)
α(°)	90.00	90.00	90.00
β (°)	94.445(9)	109.376(3)	93.021(3)
γ(°)	90.00	90.00	90.00
Volume($Å^3$)	1437.0(3)	1742.76(9)	4883.7 (3)
Z	4	4	12
D_c (g/cm^{-3})	1.378	1.430	1.482
μ (mm^{-1})	1.044	0.879	0.942
F (000)	624.0	784	2256
θ rang (°C)	2.96–26.02	3.22–25.99	2.934–25.993
Reflections collected	5284	6553	25231
Reflections unique	2826	2849	9619
Parameters	174	228	652
Goodness-of-fit on F^2	1.066	1.041	1.059
R_1, wR_2(all data)	0.0626,0.1545	0.0481, 0.0915	0.1036, 0.1449
R1, wR2 [$I > 2\sigma(I)$]	0.0497,0.1362	0.0392, 0.0991	0.0580, 0.1165
Larg.peak/hole (e. Å)	0.438/-0.617	0.395/−0.419	0.404/−0.469
CCDC no	1026164	1005424	1005425

Table 3
Selected bond lengths (Å) and angles (°) for compounds **b**, **d5** and **d6**.

$C_{16}H_{18}FeO_2$ **(b)**			
Bond lengths			
O1–C9	1.1923(69)	C5–C6	1.4620(49)
C6–C7	1.3303(52)	C7–C9	1.5002(72)
C9–O2	1.2985(75)	O2–C10	1.4739(72)
Bond angles			
C6–C5–Fe1	124.213(235)	C7–C6–C5	129.126(335)
O1–C9–O2	122.017(557)	O1–C9–C7	123.1314(480)
O2–C9–C7	114.650(474)	C9–O2–C10	116.874(461)
$C_{21}H_{21}FeNO_2$ (**d5**)			
Bond lengths			
O1–C13	1.2306(28)	C1–C11	1.4607(33)
C11–C12	1.3344(33)	N1–C13	1.3607(24)
N1–C14	1.4159(30)	C12–C13	1.4955(32)
H1–O1	2.1179(14)		
Bond angles			
C11–C1–Fe1	125.484(154)	C12–C11–C1	128.023(293)
O1–C13–N1	120.996(174)	O1–C13–C12	121.030(196)
N1–C13–C12	117.970(186)	C13–N1–C14	127.060(182)
N1–H1···O1	158.238(136)		
$C_{20}H_{18}FFeNO$ (**d6**)			
Bond lengths			
O1–C9	1.2416(43)	C5–C6	1.4665(48)
C6–C7	1.3381(48)	C7–C9	1.5011(49)
C9–N1	1.3470(46)	N1–C10	1.4227(44)
H3A-O1	2.1320(25)	H1–O2	2.0351(24)
H2A-O3	2.0931(23)		
Bond angles			
C6–C5–Fe1	128.031(255)	C7–C6–C5	128.744(325)
O1–C9–N1	122.264(327)	O1–C9–C7	119.179(315)
N1–C9–C7	118.595(295)	C9–N1–C10	126.055(282)
N3–H3A···O1	160.006(221)	N1–H1···O2	156.328(188)
N2–H2A···O3	154.434(187)		

centrifuged at 2000 rpm for 5 min. The pellet was then resuspended in 500 μL of staining solution (containing 5 μL Annexin V-PE and 5 μL PI in Binding Buffer), mixed gently and incubated for 15 min at room temperature (15–25 °C) in dark. The samples were then read in a FACS calibur flow cytometer (USA). The excitation wavelength is 488 nm and the emission wavelength are 525 nm for FITC. The excitation wavelength is 535 nm and the emission wavelength are 615 nm for PI-DNA. Analyses were performed by

Table 4
Antitumor activity (IC_{50}) of the title compounds.

Structure	Comp. no	R	IC_{50} [a] (μM)	
			B16–F10	A549
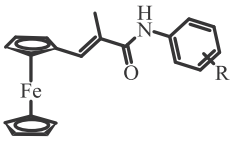	**d1**	H	0.17	15.6
	d2	4-CH_3	48.5	18.5
	d3	3-CH_3	28.6	2.1
	d4	4-OCH_3	0.46	36.4
	d5	3-OCH_3	>50	18.5
	d6	4-F	>50	39.7
	d7	3-F	>50	9.3
	d8	4-Cl	>50	9.9
	d9	3-Cl	>50	32.5
	d10	4-Br	>50	48.5
	d11	3-Br	12.8	28.1
	d12	4-CF_3	>50	16.4
	d13	3-CF_3	>50	13.6
	d14	4-OCF_3	>50	9.8
	d15	3-OCF_3	>50	11.7
	d16	3,5-di-CH_3	>50	28.2
	d17	3,5-di-OCH_3	>50	>50
	Celecoxib[b]	/	15.22	16.03

[a] Antiproliferation activity and cytotoxicity was measured using the MTT assay. Errors were in the range of 5–10% of the reported values, from three different assays.
[b] Used as a positive control.

the software supplied in the instrument [32].

3. Results and discussion

3.1. Chemistry

The synthesis of the title compounds **d1-17** was illustrated in Scheme 1. A Wittig reaction of ferrocenecarboxaldehyde with (carbethoxyethylidene) triphenylphosphorane led to the formation of compound **b** which was hydrolyzed by using sodium hydroxide to yield the (*E*)-2-methyl-3-ferrocenylacrylic acid precursor **c**. The final amides were obtained by amide coupling reaction of compound **c** with different substituted anilines at the presence of EDCI and HOBt.

3.2. Structural results from single crystal X-ray diffraction

Single crystals of compounds **b**, **d5** and **d6** were grown by slow evaporation from DCM/petroleum ether solution. Single crystal structures of compounds **b**, **d5** and **d6** were shown in Figs. 1–3, respectively.

Compound **b** is crystallized as dark-red crystal in the monoclinic space group $P2_1/c$. The principal dimensions are arcylic ester C=C 1.331 Å, C=O 1.192 Å, O–C=O 119.02°. The average bond length of Fe1–C (Cp1-5) is 2.045 Å, which is comparable to the corresponding one (2.036 Å) of another five-membered ring (Cp12-16). Among

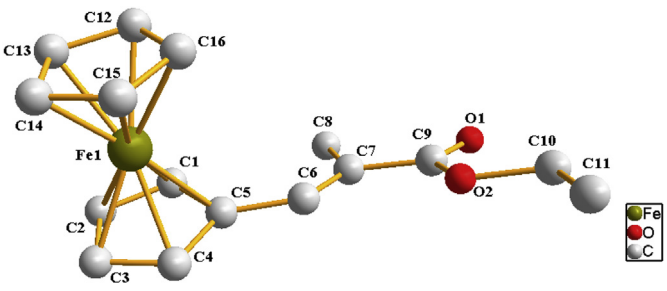

Fig. 1. X-ray structure of compound **b**.

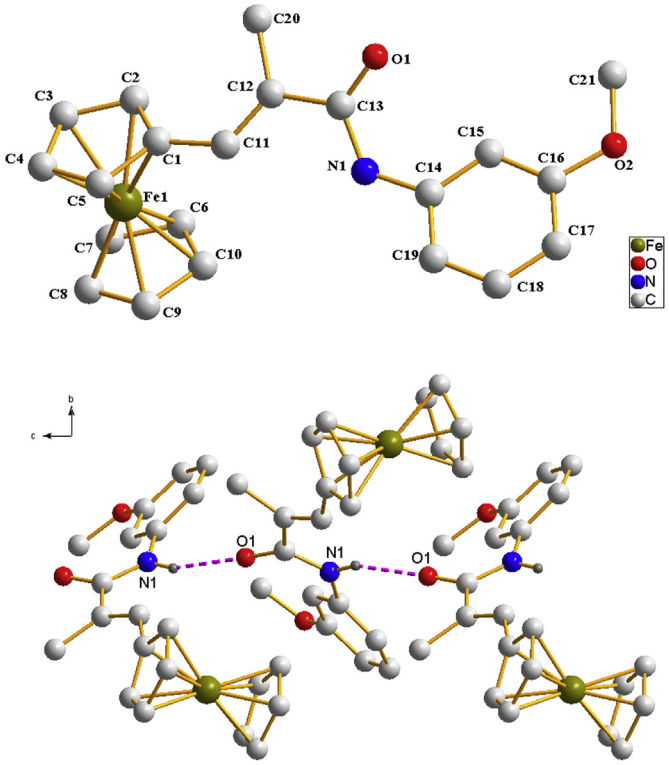

Fig. 2. X-ray structure of compound **d5**.

the ten Fe–C bonds, the Fe1–C5 bond length (2.058 Å) of the carbon atom bearing the double bond is the longest bond length, a little bit longer than the average bond length; and the shortest Fe–C (Cp) separation is 2.033 Å(Fe1–C4). As the character of other ferrocene compounds, the Fe-Cp0 (Cp^0 = centroids of Cp rings) separations are the same, 1.647 Å. The Cp0-Fe-Cp0 angle (179.23°) deviates slightly from linearity.

In the case of compound **d5**, it also crystallizes in the monoclinic space group $P2_1/c$. The principal dimensions are carboxylate ester C=O 1.231 Å, *N*–C=O 121.00°. The average bond length of Fe1–C (Cp1-5) is 2.041 Å, which is comparable to the corresponding one (2.038 Å) of another five-membered ring (Cp6-10). As well as compound **b**, the Fe1–C1 bond length (2.060 Å) of the carbon atom bearing the double bond is the longest bond length among the ten Fe–C bonds, a little bit longer than the average bond length; and the shortest Fe–C (Cp) separation is 2.026 Å(Fe1–C5).As the character of other ferrocene compounds, the Fe-Cp0 separations are 1.645 and 1.649 Å. The Cp0-Fe-Cp0 angle (178.80°) deviates slightly from linearity, indicating that this angle's deviation rate from linearity is greater than that of compound **b**.

Compound **d6** crystallizes in the monoclinic space group $P2_1/n$ with three independent molecules in the asymmetric unit. There are some differences among the three molecules. The principal dimensions are carboxylate ester C9=O1 1.242 Å, C29 = O2 1.237 Å, C49 = O3 1.244 Å and *N*–C=O with the value of 122.26°, 120.24° and 121.83°. The average distances between the Fe centre and each carbon atom of its Cp rings in the molecules are 2.032–2.038 Å. This distance is nearly identical to the analogs average distance found in ferrocene. The shortest Fe–C(Cp) separation is to C37, with value of 2.128(4) Å. As well as the above compounds, the Fe1–C5 bond length (2.059 Å) of the carbon atom bearing the double bond is the longest bond length among the Fe–C bonds, a little bit longer than the average bond length. The Cp^0-Fe-Cp^0 angles both deviate somewhat from linearity (179.66, 179.17 and 178.04°).

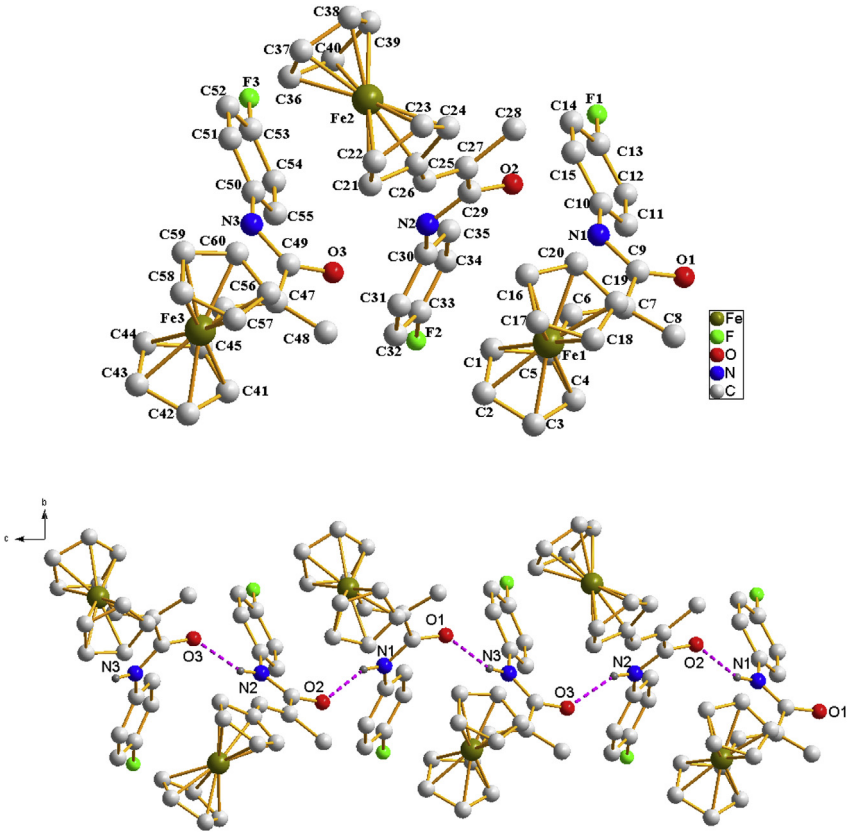

Fig. 3. X-ray structure of compound **d6**.

As can be seen from the above data (Figs. 2 and 3), this kind of ferrocenyl-*N*-acrylamide compounds can form intermolecular hydrogen bond between nitrogen atom of the amide group and the oxygen atom of another amide group. The intermolecular H bonds between adjacent molecules lead to a 1D chain structure. This bonding behavior may be helpful when this kind of compounds interact with the amino acid residues of their potential target *in vitro*.

3.3. Antitumor activity

The effect of substituents on the phenyl ring was investigated. (*E*)-2-methyl-3-ferrocenyl-*N*-acrylamide derivatives were evaluated for their *in vitro* antitumor activity against two tumor cell lines B16−F10 and A549 using MTT assay and were compared with the reference compound celecoxib. The result is summarized in Table 4. Brief structure-activity for potency of **d1**-**d17** is as follows.

When the compounds **d1**-**d17** were tested against B16−F10, it can be seen that the non-substituted compound **d1** exhibited the most potent antitumor activity with the IC_{50} value of 0.17 μM. The 4- and 3-positions of the phenyl ring were then interrogated with similar substituents based on **d1** as a template. The intent was to find out a substituent at the 2- or 3-position which can improve the antitumor activity. First, different kind of electron-donating and electron-withdrawing groups were introduced onto the 4- and 3-positions. It could be seen that the introduction of electron-withdrawing groups like F, Cl, Br, CF_3 and OCF_3 onto the 4-position lead to a dramatic decrease of antitumor activity. In terms of the 3-position, it was almost the same as the 4-position except the 3-Br (**d11**). Then, the 4- and 3-positions were experimented with electron-donating groups such as CH_3 and OCH_3. When CH_3 was probed at each of 4- or 3-position, the antitumor activity could be retained to some extent. A 4-OCH_3 substituent gave rise to analogue **d4**, exhibited comparable activity to the original compound **d1**. Interestingly, the 3-OCH_3 substituted one (**d5**) was almost inactive. This may be attributed to the decreased binding affinity produced by these substituents to the target protein.

On the other hand, most of the compounds exhibited moderate activity when tested against A549 cell line. The SAR was not so tight as we observed in terms of B16−F10. Compounds **d1**, **d3**, **d7**, **d8**, **d13**, **d14** and **d15** showed superior activity to celecoxib. In particular, compound **d3** with *m*-methyl group displayed the most potential in A549 cell line. Compounds **d7**, **d8** and **d15**, which have halogen substituent groups also exhibited good antitumor in A549 cell line. The introduction of 3-methyl, 3-fluoro, 3-trifluoromethyl and 3-trifluoromethoxy groups on the phenyl ring significantly enhanced the antitumor activity with the non-substituted compound **d1**. In addition, the introduction of 4-chloro, 4-trifluoromethoxy groups on the phenyl ring can also enhance the antitumor activity with the non-substituted compound **d1**. It was quite different from the result when tested against B16−F10.

3.4. Analysis of apoptosis by fluorescence-activated cell sorting

We evaluated the effect of compound **d1** on B16−F10 cell apoptosis to determine whether the cell death was related to cell apoptosis. B16−F10 cells were treated with different concentrations (2 μM, 4 μM, 8 μM and 16 μM) of **d1** for 24 h and analyzed cells for changes in apoptotic markers with a flow cytometer *in vitro*. As shown in Fig. 4, we can see that each concentration of compound

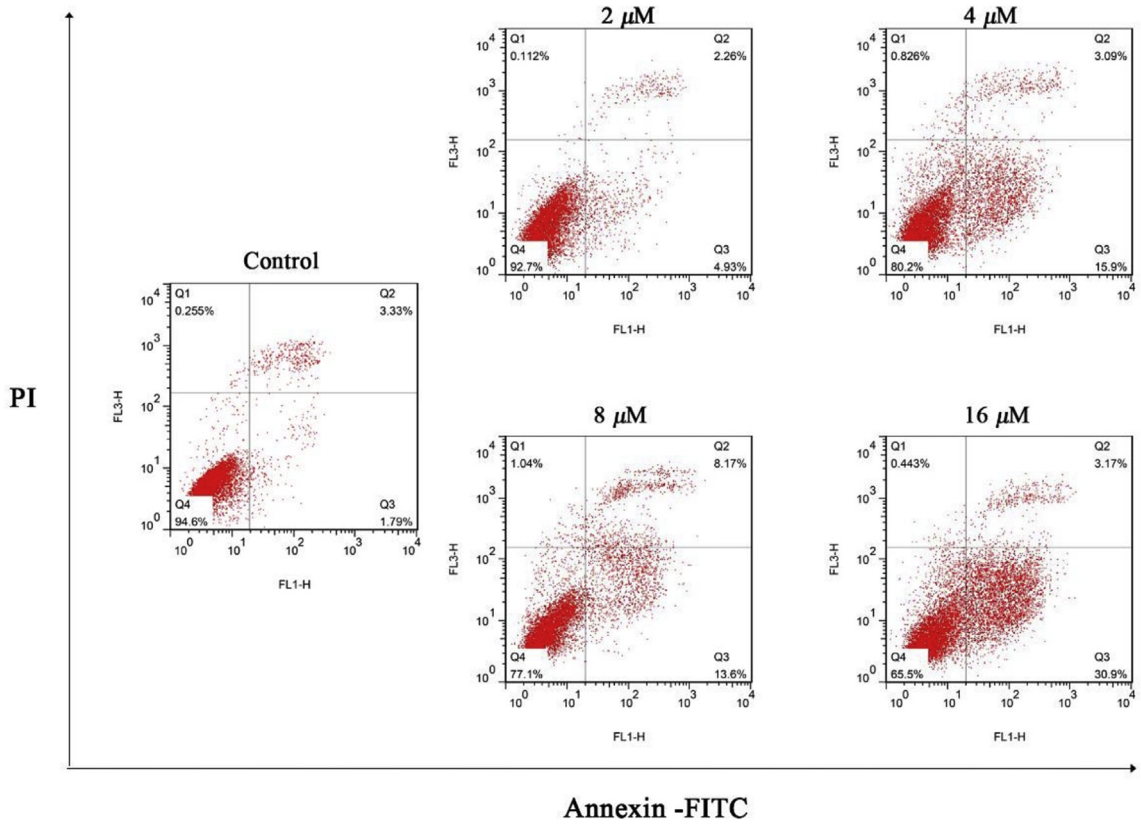

Fig. 4. Representative flow cytometric histograms of apoptotic B16–F10 cells after 24 h treatment with different dose of compound **d1**. The cells were harvested and labeled with Annexin-V-FITC and PI and then analyzed by flow cytometry.

d1 induced an accumulation of annexin-V positive cells in comparison with the control. Furthermore, the percentage of apoptotic cells was obviously increased at a dose-dependent manner. The percentage of apoptotic cell were 4.93%, 15.9%, 13.6%, 30.9% respectively, corresponding to the concentration of 2, 4, 8, 16 μM. These data indicated that compound **d1** might exert its antitumor activity by inducing cell apoptosis in B16–F10 cells.

4. Conclusion

In summary, seventeen (*E*)-2-methyl-3-ferrocenyl-*N*-acrylamide derivatives (**d1-17**) were synthesized and characterized. Among them, the structures of **d5**, **d6** and **b** were further determined by X-ray single crystal diffraction. Compounds **d1-17** were evaluated for their *in vitro* antitumor activity against B16–F10 and A549 cell lines. Compound **d1** with no substituted group on the phenyl ring exhibited the most potent antitumor activity with an IC_{50} value of 0.17 μM against B16–F10 cell line. Introduction of methyl, methoxy, halogen, trifluoromethyl and trifluoromethoxy group on the *meta*- or *para*-position can significantly decrease the antitumor activity. In addition, compound **d3** with 3-methyl group on the phenyl ring exhibited the most potent antitumor activity with an IC_{50} value of 2.1 μM against A549 cell line. Furthermore, flow cytometry assay results indicated that compound **d1** could induce apoptosis in B16–F10 cells. These results revealed that this novel (*E*)-2-methyl-3-ferrocenyl-*N*-acrylamide derivative could be a potential antitumor drug candidate.

Supplementary material

CCDC 1026164, 1005424 and 1005425 contain the supplementary crystallographic data for compounds **b**, **d5** and **d6**, respectively. These data can be obtained free of charge from The Cambridge Crystallographic Data Centre via www.ccdc.cam.ac.uk/data_request/cif.

Acknowledgements

This work was supported by the Key Scientific and Technological Project of Anhui Provincial Tobacco Company (No. 20150551007).

References

[1] R.H. Fish, G. Jaouen, Bioorganometallic chemistry: structural diversity of organometallic complexes with bioligands and molecular recognition studies of several supramolecular hosts with biomolecules, alkali-metal ions, and organometallic pharmaceuticals, Organometallics 22 (2003) 2166–2177.
[2] U. Schatzschneider, N. Metzler-Nolte, New principles in medicinal organometallic chemistry, Angew. Chem. Int. Ed. 45 (2006) 1504–1507.
[3] M. Patra, G. Gasser, A. Pinto, K. Merz, I. Ott, J.E. Bandow, N. Metzler-Nolte, Synthesis and biological evaluation of chromium bioorganometallics based on the antibiotic platensimycin lead structure, ChemMedChem 4 (2009) 1930–1938.
[4] A. Bergamo, G. Sava, Ruthenium anticancer compounds: myths and realities of the emerging metal-based drugs, Dalton Trans. 40 (2011) 7817–7823.
[5] G.S. Smith, B. Therrien, Targeted and multifunctional arene ruthenium chemotherapeutics, Dalton Trans. 40 (2011) 10793–10800.
[6] S. Top, G. Jaouen, A. Vessières, J.-P. Abjean, D. Davoust, C.A. Rodger, B.G. Sayer, M.J. McGlinchey, Chromium tricarbonyl complexes of estradiol derivatives: differentiation of α- and β-diastereoisomers using one- and two-dimensional NMR spectroscopy at 500 MHz, Organometallics 4 (1985) 2143–2150.
[7] R. Lippert, T.E. Shubina, S. Vojnovic, A. Pavic, J. Veselinovic, J. Nikodinovic-Runic, N. Stankovic, I. Ivanović-Burmazović, Redox behavior and biological properties of ferrocene bearing porphyrins, J. Inorg. Biochem. 171 (2017) 76–89.
[8] O. Buriez, J.M. Heldt, E. Labbé, A. Vessières, G. Jaouen, C. Amatore, Reactivity and antiproliferative activity of ferrocenyl-tamoxifen adducts with cyclodextrins against hormone-independent breast-cancer cell lines, Chem. Eur J. 14

(2008) 8195–8203.
[9] D. Hamels, P.M. Dansette, E.A. Hillard, S. Top, A. Vessières, P. Herson, G. Jaouen, D. Mansuy, Ferrocenyl quinone methides as strong antiproliferative agents: formation by metabolic and chemical oxidation of ferrocenyl phenols, Angew. Chem. Int. Ed. vol 48 (2009) 9124–9126.
[10] X. Wu, E.R.T. Tiekink, I. Kostetski, N. Kocherginski, A.L.C. Tan, S.B. Khoo, P. Wilairat, M.L. Go, Eur. J. Pharm. Sci. 27 (2006) 175–187.
[11] D. Dive, C. Biot, Ferrocene conjugates of chloroquine and other antimalarials: the development of ferroquine, a new antimalarial, ChemMedChem 3 (2008) 383–391.
[12] Z.H. Cohan, Antibacterial and antifungal ferrocene incorporated dithiothione and dithioketone compounds, Appl. Organomet. Chem. 20 (2006) 112–116.
[13] M. Patra, G. Gasser, M. Wenzel, K. Merz, J.E. Bandow, N. Metzler-Nolte, Synthesis and biological evaluation of ferrocene-containing bioorganometallics inspired by the antibiotic platensimycin lead structure, Organometallics 29 (2010), 4312-4219.
[14] B. Maity, M. Roy, A.R. Chakravarty, Ferrocene-conjugated copper (II) dipyridophenazine complex as a multifunctional model nuclease showing DNA cleavage in red light, J. Organomet. Chem. 693 (2008) 1395–1399.
[15] B. Maity, V.S.K. Chakravarthi, M. Roy, A.A. Karande, A.R. Chakravarty, DNA photocleavage and cytotoxic properties of ferrocene conjugates, Eur. J. Inorg. Chem. 2011 (2011) 1379–1386.
[16] B. Zhou, C.L. Li, Y.Q. Hao, M.C. Johnny, Y.N. Liu, J. Li, Ferrocene tripeptide Gly-Pro-Arg conjugates: synthesis and inhibitory effects on Alzheimer's Aβ1-42 fibrillogenesis and Aβ-induced cytotoxicity in vitro, Bioorg. Med. Chem. 21 (2013) 395–402.
[17] C.W. Wei, Y. Peng, L. Zhang, Q. Huang, M. Chemg, Y.N. Liu, J. Liu, Synthesis and evaluation of ferrocenoyl pentapeptide (Fc-KLVFF) as an inhibitor of Alzheimer's $A\beta_{1-42}$ fibril formation in vitro, Bioorg. Med. Chem. Lett 21 (2011) 5818–5821.
[18] C. Roux, C. Biot, Ferrocene-based antimalarials, Future Med. Chem. 4 (2012) 783–797.
[19] G. Jaouen, A. Vessières, S. Top, Ferrocifen type anticancer drugs, Chem. Soc. Rev. 44 (2015) 8802–8817.
[20] M. Patra, G. Gasser, The medicinal chemistry of ferrocene and its derivatives, Nat. Rev. Chem. 1 (2017) 1–12.
[21] K. Kowalski, Recent developments in the chemistry of ferrocenyl secondary natural product conjugates, Coord. Chem. Rev. 366 (2018) 91–108.
[22] G. Jaouen, N. Metzler-Nolte, Topics in Organometallic Chemistry, Medicinal Organometallic Chemistry, Springer, Berlin, 2010.
[23] A.I. Gutiérrez-Hernández, J.G. López-Cortés, M.C. Ortega-Alfaro, M.T. Ramírez-Apan, J. de J. Cázares-Marinero, R.A. Toscano, Ferrocenylselenoamides: synthesis, characterization and cytotoxic properties, J. Med. Chem. 55 (2012) 4652–4663.
[24] A.J. Salmon, M.L. Williams, Q.K. Wu, J. Morizzi, D. Gregg, S.A. Charman, D. Vullo, C.T. Supuran, S.A. Poulsen, Metallocene-based inhibitors of cancer-associated carbonic anhydrase enzymes IX and XII, J. Med. Chem. 55 (2012) 5506–5517.
[25] M. Patra, K. Ingram, V. Pierroz, S. Ferrari, B. Spingler, J. Keiser, G. Gasser, Ferrocenyl derivatives of the anthelmintic praziquantel: design, synthesis, and biological e valuation, J. Med. Chem. 55 (2012) 8790–8798.
[26] P. Marzenell, H. Hagen, L. Sellner, T. Zenz, R. Grinyte, V. Pavlov, S. Daum, A. Mokhir, Aminoferrocene-based prodrugs and their effects on human normal and cancer cells as well as bacterial cells, J. Med. Chem. 56 (2013) 6935–6944.
[27] D. Huber, H. Hubner, P. Gmeiner, 1,1' -Disubstituted ferrocenes as molecular hinges in mono- and bivalent dopamine receptor ligands, J. Med. Chem. 52 (2009) 6860–6870.
[28] S. Daum, V.F. Chekhun, I.N. Todor, N.Y. Lukianova, Y.V. Shvets, L. Sellner, K. Putzker, J. Lewis, T. Zenz, I.A.M. de Graaf, G.M.M. Groothuis, A. Casini, O. Zozulia, F. Hampel, A. Mokhir, Improved synthesis of N-benzylamino-ferrocene-based prodrugs and evaluation of their toxicity and antileukemic activity, J. Med. Chem. 58 (2015) 2015–2024.
[29] M.H. Kunzmann, N.C. Bach, B. Bauer, S. Sieber, α-Methylene-g-butyrolactones attenuate Staphylococcus aureus virulence by inhibition of transcriptional regulation, Chem. Sci. 5 (2014) 1158–1167.
[30] X.F. Huang, J.F. Tang, J.L. Ji, X.L. Wang, B.F. Ruan, Synthesis, characterization and antitumor activity of novel amide derivatives containing ferrocenyl pyrazol-moiety, J. Organomet. Chem. 706–707 (2012) 113–123.
[31] X.F. Huang, L.Z. Wang, L. Tang, Y.X. Lu, F. Wang, G.Q. Song, B.F. Ruan, Synthesis, characterization and antitumor activity of novel ferrocene derivatives containing pyrazolyl-moiety, J. Organomet. Chem. 749 (2014) 157–162.
[32] Y. Guo, S.Q. Wang, Z.Q. Ding, J. Zhou, B.F. Ruan, Synthesis, characterization and antitumor activity of novel ferrocene bisamide derivatives containing pyrimidine-moiety, J. Organomet. Chem. 851 (2017) 150–159.
[33] R.S. Yao, X.Q. Lu, Q.X. Guan, L. Zheng, X. Lu, B.F. Ruan, Synthesis and biological evaluation of some novel resveratrol amide derivatives as potential anti-tumor agents, Eur. J. Med. Chem. 62 (2013) 222–231.
[34] B.F. Ruan, S.Q. Wang, X.L. Ge, R.S. Y, Synthesis of resveratrol acrylamides derivatives and biological evaluation of their anti-proliferative effect on cancer cell lines, Lett. Drug Des. Discov. 11 (2014) 2–9.
[35] B.F. Ruan, W.W. Ge, H.J. Cheng, H.J. Xu, Q.S. Li, X.H. Liu, Resveratrol-based cinnamic ester hybrids: synthesis, characterization, and anti-inflammatory activity, J. Enzym. Inhib. Med. Chem. 32 (2017) 1282–1290.
[36] G.M. Sheldrick, SHELXTL V5.1 Software Reference Manual, Bruker AXS, Inc., Madison, WI, USA, 1997.
[37] X. Chen, C. Plasencia, Y. Hou, N. Neamati, Synthesis and biological evaluation of dimeric RGD peptide-paclitaxel conjugate as a model for integrin-targeted drug delivery, J. Med. Chem. 48 (2005) 1098–1106.